# BrainUSL: Unsupervised Graph Structure Learning for Functional Brain Network Analysis

Pengshuai Zhang[1,2], Guangqi Wen[1,2], Peng Cao[1,2,3(✉)], Jinzhu Yang[1,2,3], Jinyu Zhang[1,2], Xizhe Zhang[4], Xinrong Zhu[5], Osmar R. Zaiane[6], and Fei Wang[5(✉)]

[1] Computer Science and Engineering, Northeastern University, Shenyang, China
caopeng@cse.neu.edu.cn
[2] Key Laboratory of Intelligent Computing in Medical Image of Ministry of Education, Northeastern University, Shenyang, China
[3] National Frontiers Science Center for Industrial Intelligence and Systems Optimization, Shenyang, China
[4] Biomedical Engineering and Informatics of Nanjing Medical University, Nanjing, China
[5] Early Intervention Unit, Department of Psychiatry, Affiliated Nanjing Brain Hospital, Nanjing Medical University, Nanjing, China
fei.wang@yale.edu
[6] Amii, University of Alberta, Edmonton, AB, Canada

**Abstract.** The functional connectivity (FC) between brain regions is usually estimated through a statistical dependency method with functional magnetic resonance imaging (fMRI) data. It inevitably yields redundant and noise connections, limiting the performance of deep supervised models in brain disease diagnosis. Besides, the supervised signals of fMRI data are insufficient due to the shortage of labeled data. To address these issues, we propose an end-to-end unsupervised graph structure learning method for sufficiently capturing the structure or characteristics of the functional brain network itself without relying on manual labels. More specifically, the proposed method incorporates a graph generation module for automatically learning the discriminative graph structures of functional brain networks and a topology-aware encoding module for sufficiently capturing the structure information. Furthermore, we also design view consistency and correlation-guided contrastive regularizations. We evaluated our model on two real medical clinical applications: the diagnosis of Bipolar Disorder (BD) and Major Depressive Disorder (MDD). The results suggest that the proposed method outperforms state-of-the-art methods. In addition, our model is capable of identifying associated

P. Zhang and G. Wen—Contribute equally to this work.

**Supplementary Information** The online version contains supplementary material available at https://doi.org/10.1007/978-3-031-43993-3_20.


H. Greenspan et al. (Eds.): MICCAI 2023, LNCS 14227, pp. 205–214, 2023.
https://doi.org/10.1007/978-3-031-43993-3_20

biomarkers and providing evidence of disease association. To the best of our knowledge, our work attempts to construct learnable functional brain networks with unsupervised graph structure learning. Our code is available at https://github.com/IntelliDAL/Graph/tree/main/BrainUSL.

**Keywords:** Functional connectivity analysis · Graph structure learning · Unsupervised learning · fMRI

## 1 Introduction

Recent studies have shown that rs-fMRI based analysis for brain functional connectivity (FC) is effective in helping understand the pathology of brain diseases [8,17,25]. The functional connectivity in the brain network can be modeled as the graph where nodes denote the brain regions and the edges represent the correlations between those regions [6]. Hence, the brain disease identification can be seen as the graph classification with the refined graph structures [28].

The representation learning of brain network heavily relies on the graph structure quality. The existing brain network construction methods [16,23] are often noisy or incomplete due to the inevitably error-prone data measurement or collection. The noisy or incomplete graphs often lead to unsatisfactory representations and prevent us from fully understanding the mechanism underlying the disease. In pursuit of an optimal graph structure for graph classification, recent studies have sparked an effort around the central theme of Graph Structure Learning (GSL), which aims to learn an optimized graph structure and corresponding graph representations. However, most works for GSL rely on the human annotation, which plays an important role in providing supervision signals for structure improvement. Since the fMRI data is expensive and limited, unsupervised graph structure learning is urgently required [1,4,14]. Moreover, disease interpretability is essential as it can help decision-making during diagnosis.

Considering the above issues, we aim to discover useful graph structures via a learnable graph structure from the BOLD signals instead of measuring the associations between brain regions by a similarity estimation. In this paper, we propose an end-to-end unsupervised graph structure learning framework for functional brain network analysis (BrainUSL) directly from the BOLD signals. The unsupervised graph structure learning consists of a graph generation module and the topology-aware encoder. We propose three loss functions to constrain the graph structure learning, including the sparsity-inducing norm, the view consistency regularization and the correlation-guided contrastive loss. Finally, the generated graph structures are used for the graph classification. We evaluate our model on two real medical clinical applications: Bipolar Disorder diagnosis and Major Depressive Disorder diagnosis. The results demonstrate that our BrainUSL achieves remarkable improvements and outperforms state-of-the-art methods. The main contributions of this paper are summarized below:

- We propose an end-to-end unsupervised graph structure learning method for functional brain network analysis.
- We propose the correlation-guided contrastive loss to model the correlations between graphs by defining the sample correlation estimation matrix.

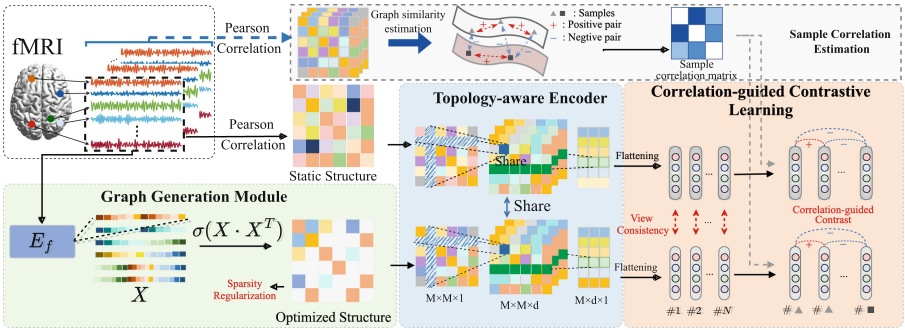


**Fig. 1.** Illustration of the proposed BrainUSL. The unsupervised graph structure learning module consists of a graph generation module for generating optimized sparsity-induced graph structures, a topology-aware encoder for capturing the essential topological representation and a correlation-guided contrastive learning for exploiting discriminative and sparse graph structures. Then, three loss functions are proposed for guiding the procedure of graph structure learning. Finally, the generated graph structure for each subject and the topology-aware encoder are further used for the downstream classification.

- Our method provides a perspective for disease interpretable analysis and association analysis between BD and MDD.
- The experimental results demonstrate the advantage of the proposed method in brain disorder diagnosis.

## 2 Method

The constructed graph structure of brain network in existing works are often noisy or incomplete. To address this issue, we propose a novel unsupervised graph structure learning method, including the graph generation module for generating optimized sparsity-induced graphs and the topology-aware encoder for capturing the topological information in graphs, as illustrated in Fig. 1. Then, we propose a new objective function for unsupervised graph structure learning from the perspectives of constraining structure sparsity as well as view consistency and preserving discriminative patterns at the same time.

### 2.1 Graph Generation Module

To exploit the information in fMRI signals for generating the optimized sparsity-induced graph structure, we propose a graph generation module, which containing a graph generation module contains BOLD signal feature aggregation ($E_f$) with a stack of convolutional layers [7] for learning the low-dimensional BOLD signal features. The feature is learned as follows:

$$E_f^{(l+1)}(u) = \sum_{s=0}^{U-1} E_f^{(l)}(u-s) * \mathcal{K}^{(l)}(s), \tag{1}$$

where $\mathcal{K}^{(l)}$ is a convolutional kernel of $l$-th layer with a kernel size of $U$ and $u$ denotes the BOLD signal element in a brain region of the input $x$. With the feature learned by $E_f$, we generate the optimized graph $A_G$ by calculating the correlation among the nodes.

### 2.2 Topology-Aware Encoder

The graph topological information is crucial for graph embedding learning. Motivated by BrainNetCNN [5], we propose a Topology-aware Encoder for exploiting the spatial locality in the graph structure through a hierarchical local (edge)-to-global (node) strategy by aggregating the embeddings of the connections associated with the nodes at the two ends of each edge. The topology-aware encoder involves an operator of *edge aggregation* ($E_g$) with multiple cross-shaped filters for capturing the spatial locality in the graph and *node aggregation* ($E_n$) for aggregating the associated edge. The *cross-shaped filters* in edge aggregation involve a combination of $1 \times M$ and $M \times 1$ basis filters with horizontal and vertical orientations, which are defined as:

$$H_g = E_g(A) = \sum_{i=0}^{M} \sum_{j=0}^{M} A^{(i,\cdot)} w^r + A^{(\cdot,j)} w^h, \tag{2}$$

where $w^r \in \mathbb{R}^{1\times M}$ and $w^h \in \mathbb{R}^{M\times 1}$ denote the learned vectors of the horizontal and vertical convolution kernel, $M$ denotes the number of ROIs, $A$ and $H_g$ denote the adjacency matrix and the edge embeddings. With the learned edge embeddings, we further learn the node embeddings by aggregating the associated edges with the nodes with a learnable layer. More specifically, the node aggregation takes the edge embedding as the inputs and obtains the node embedding from a node-wise view by a 1D convolutional filter. The node aggregation is defined as:

$$H_n = E_n(H_g) = \sum_{i=1}^{M} H_g^{(i,\cdot)} w^n, \tag{3}$$

where $H_n \in \mathbb{R}^{M\times d}$ is the node embedding, and $w^n \in \mathbb{R}^{1\times M}$ is the learned vector of the filter, and $d$ is the dimensionality of the node embeddings.

### 2.3 Objective Functions

To better exploit the graph structure, we design three loss functions including a sparsity-inducing norm, a view consistency regularization and a correlation-guided contrastive loss. We assume that the sparsity of the generated graphs allows for the preservation of the important edges and removal of noise. To achieve this, we utilize an $l_1$ norm to remove the irrelevant connections and preserve the sparsity of the generated graphs.

Furthermore, we introduce a view consistency regularization to ensure the consistency of two views by maximizing the agreement between the node embeddings learned from the fixed graph structure $A_P$ and learnable graph structure

$A_G$. The view consistency regularization is defined as $L_{vc} = \sum_{i=1}^{N} sim(e_i, \hat{e}_i)$, where $sim(\cdot, \cdot)$ is a cosine similarity measure, $N$ denotes the number of samples, $\hat{e}_i$ and $e_i$ represent the $i$-th graph embeddings from $A_P$ and $A_G$.

The motivation of contrastive learning is to capture the graph embeddings by modeling the correlations between graphs [24]. However, it produces bias depending on the simple data augmentations, which can degrade performance on downstream tasks. Hence, we introduce the graph correlation estimation by graph kernel [27] to construct the correlation matrix $S \in N \times N$. Then, we binarize the matrix by a simple thresholding with a threshold value $\theta$. If $S_{ij} \geq \theta$, we set $S_{ij}$ to 1, which indicates that the $i$-th and $j$-th samples are regarded as a positive sample pair. Otherwise, $S_{ij}$ is set to 0, indicating they are considered as a negative sample pair. With the estimated positive and negative pairs, the correlation-guided contrastive loss is defined as:

$$L_{cc} = -\sum_{i=1}^{N} \log \frac{\sum_{S_{ij}=1} \exp(sim(e_i, e_j)/\tau)}{\sum_{j=1}^{N} \mathbb{1}_{i \neq j} \exp(sim(e_i, e_j)/\tau)}, \tag{4}$$

where $\mathbb{1}(\cdot) = \{0, 1\}$ is an indicator function, and $\tau$ is a temperature factor to control the desired attractiveness strength.

The final objective function is formulated as:

$$L = L_{vc} + \alpha L_{cc} + \beta \left\| A_G \right\|_1, \tag{5}$$

where $\alpha$ and $\beta$ are the trade-off hyper-parameters. Finally, based on the generated graphs and pre-trained topology-aware encoder, we leverage the multi-layer perceptron (MLP) with the cross-entropy loss for the graph classification.

## 3 Experiments and Results

### 3.1 Dataset and Experimental Details

We evaluated our BrainUSL on a private dataset constructed from Nanjing Medical University (NMU) for BD and MDD diagnosis by repeating the 5-fold cross-validation 5 times with different random seeds. We deal with the original fMRI data by dpabi [20] and divide the whole brain into 116 brain regions based on Automated Anatomical Labeling (AAL) for analysis, which included spatial normalization to Echo Planar Imaging (EPI) template of standard Montreal Neurological Institute (MNI) space (spatial resolution 3 mm × 3 mm × 3 mm), spatial and temporal smoothing with a 6 mm × 6 mm × 6 mm Gaussian kernel and filter processing with adopting 0.01–0.08 Hz low-frequency fluctuations to remove interference signals. The dataset includes 172 health controls (104 females and 68 males, aged 24.89 ± 7.14 years, range 18–43 years), 127 MDDs (90 females and 37 males, age range 17–34 years) and 102 BDs (76 females and 26 males, age range 16–32 years), who were scanned at a single site with identical inclusion and exclusion criteria.

**Table 1.** Classification results on the diagnosis of BD and MDD. $L_{vc}$: view consistency regularization; $L_{cc}$: correlation-guided contrastive loss.

| Methods | HC vs. BD | | | | HC vs. MDD | | | |
|---|---|---|---|---|---|---|---|---|
| | ACC (%) | AUC (%) | SEN (%) | SPEC (%) | ACC (%) | AUC (%) | SEN(%) | SPEC (%) |
| FC + SVM [21] | 73.2 | 70.8 | 65.3 | 72.9 | 68.1 | 67.5 | 66.5 | 75.4 |
| FC + RF [21] | 67.7 | 60.2 | 60.1 | 65.0 | 63.4 | 59.8 | 63.8 | 66.1 |
| GroupINN [22] | 67.9 | 63.3 | 62.8 | 67.1 | 66.8 | 65.3 | 63.1 | 65.8 |
| ASD-DiagNet [2] | 73.3 | 70.1 | 58.5 | 79.6 | 68.2 | 66.7 | 60.2 | 74.3 |
| MVS-GCN [18] | 66.9 | 64.2 | 62.1 | 73.5 | 68.3 | 68.2 | 63.8 | 61.2 |
| ST-GCN [3] | 67.1 | 57.5 | 56.6 | 73.5 | 58.1 | 52.3 | 53.3 | 55.1 |
| BrainNetCNN [5] | 73.3 | 71.7 | 64.1 | 79.3 | 69.4 | 68.4 | 61.5 | 75.2 |
| BrainUSL - w/o $l_1$ | 75.5 | 73.6 | **65.2** | 82.0 | 75.4 | 74.2 | 67.5 | 81.0 |
| BrainUSL - w/o $L_{vc}$ | 75.6 | 72.7 | 62.8 | 82.7 | 73.8 | 73.1 | **69.5** | 76.7 |
| BrainUSL - w/o $L_{cc}$ | 75.0 | 71.7 | 59.1 | 84.3 | 74.1 | 73.1 | 65.4 | 80.8 |
| BrainUSL (Ours) | **77.3** | **74.4** | 63.0 | **85.7** | **76.7** | **75.3** | 67.6 | **82.6** |
| BrainUSL - BD | – | – | – | – | 75.2 | 74.1 | 67.8 | 80.5 |
| BrainUSL - MDD | 76.4 | 73.7 | 63.2 | 84.2 | – | – | – | – |

### 3.2 Classification Results

We compare our BrainUSL with state-of-the-art models in terms of Accuracy (ACC), Area Under the Curve (AUC), Sensitive (SEN) and Specificity (SPEC). The comparable methods can be grouped into two categories: traditional methods including FC+SVM/RF [21] and deep learning methods including GroupINN [22], ASD-DiagNet [2], MVS-GCN [18], ST-GCN [3] and BrainNetCNN [5].

**Comparison with SOTA.** Compared with state-of-the-art methods, the proposed BrainUSL generally achieves the best performance on MDD and BD identification, the results are shown in Table 1. Specifically, the results show that our BrainUSL yields the best ACC and AUC results on MDD (ACC = 76.7% and AUC = 75.3%) and BD (ACC = 77.3% and AUC = 74.4%), compared to the existing brain disease diagnosis approaches. Moreover, Fig. 2 illustrates the influence of the pre-training epochs of BrainUSL on the classification performance. It can be found that the performance improves with the pre-training epochs increasing until 40/60 epochs for BD/MDD, which demonstrates that more pre-training epochs help capture accurate structural representation. In addition, the similar sparsity patterns are observed for both the diagnosis of two disorders. The results demonstrate that our generated graphs are more discriminative than the graphs constructed by pearson correlation coefficient, which confirms that the quality of the graph structure is critical for functional brain network representation learning, and noisy or redundant connections in brain network impede understanding of disease mechanisms.

**Ablation Study.** There are three parts in our final objective function. Next, we perform a sequence of ablation studies on the three parts of our model. As

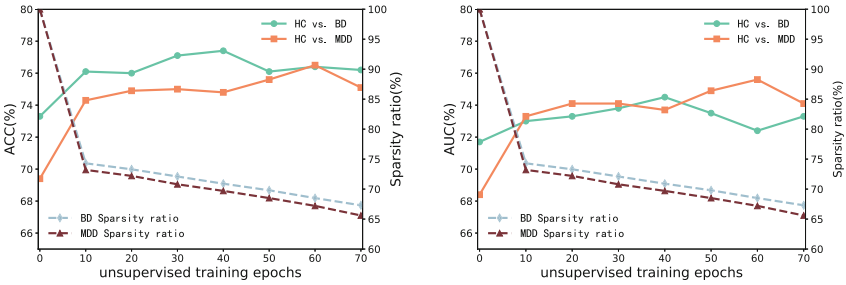


(a) The impact curve of ACC (b) The impact curve of AUC

**Fig. 2.** The impact of unsupervised training epochs.

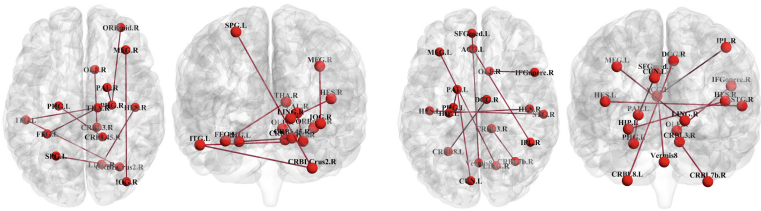

(a) Top-10 connections of BD (b) Top-10 connections of MDD

**Fig. 3.** Illustration of discriminative connections for brain disease diagnosis.

shown the third part in Table 1, all the proposed loss functions obviously improve the classification performance, showing the crucial role of the each component and the complementary one another. Therefore, our results demonstrate that the graph structure constructed in an unsupervised manner can provide the potential correlations and discriminative information between brain regions precisely.

### 3.3 Functional Connectivity Analysis

We use BrainNetViewer [19] to illustrate the discriminative top-10 connections identified by our method for brain disease diagnosis in Fig. 3. Neuroimaging studies have demonstrated that the subnetworks of SN, CEM, and DMN are often co-activated or deactivated during emotional expression task. We find that some identified connections in MDD and BD such as Frontal-Mid-R between Frontal-Sup-Medial-L and Angular-L between Thalamus-L are the key connections in DMN, CEN and SN, which demonstrates that our model can generate the discriminative brain structure and facilitate the identification of biomarkers [10–12]. Furthermore, as shown in Fig. 4, by comparing the graphs constructed by PCC and BrainUSL, it can be observed that our method produces a sparser structure for the brain network, indicating that only a small portion of the functional connections are relevant to the outcome. The results indicate that the generated

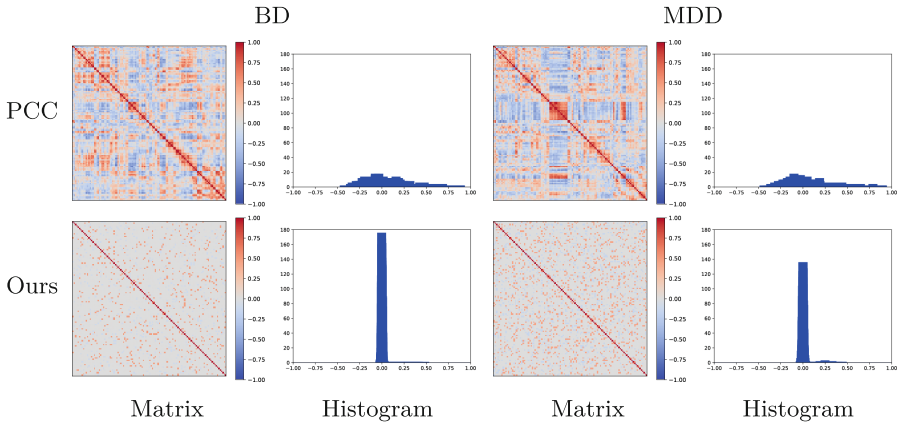


**Fig. 4.** Differences in connectivity patterns constructed by PCC (Top) and BrainUSL (Bottom). The 1st and 3rd columns indicate two examples of the generated graph structures. The 2nd and 4th columns indicate the histograms of connection strengths excluding the diagonal elements for all the subjects by PCC and our learnable manner.

graph structures via unsupervised learning can effectively reflect the intrinsic connections between brain regions caused by brain disorders.

### 3.4 Association of Brain Diseases

A number of studies [9,15] have demonstrated there exists associations between different psychiatric disorders [13], patients with one psychiatric disorder are more susceptible to other psychiatric disorders. We evaluate the association between the disorders and the transfer learning ability of our model. Specifically, We pre-train our model on one dataset, then fine-tune and evaluate it on the other dataset. The results are illustrated in the last part of Table 1. We observed that the transfer learning between two different brain disorder disease also achieve a better results compared with other methods. The result indicates that the two diseases are correlated, which is consistent with the existing study results [26]. Moreover, the results also indicate that our model learns more transferable representations and provides a perspective for the study of disease associations through transfer learning on the functional brain network analysis.

## 4 Conclusion

Due to the inevitably error-prone data measurement or collection, the functional brain networks constructed by existing works are often noisy and incomplete. To address this issue, we propose the unsupervised graph structure learning framework for functional brain network analysis (BrainUSL), which generates the sparse and discriminative graph structures according to the characteristics of the graph data itself. We conducted extensive experiments on the NMU

dataset which indicate that our BrainUSL achieves promising performance with the SOTA methods. In addition, we discuss the interpretability of our model and find discriminative correlations in functional brain networks for diagnosis.

**Acknowledgment.** This paper is supported by the National Natural Science Foundation of China (No. 62076059), the Science Project of Liaoning province (2021-MS-105) and the 111 Project (B16009).

## References

1. Chavas, J., Guillon, L., Pascucci, M., Dufumier, B., Rivière, D., Mangin, J.F.: Unsupervised representation learning of cingulate cortical folding patterns. In: Wang, L., Dou, Q., Fletcher, P.T., Speidel, S., Li, S. (eds.) MICCAI 2022, Part I. LNCS, vol. 13431, pp. 77–87. Springer, Cham (2022). https://doi.org/10.1007/978-3-031-16431-6_8
2. Eslami, T., Mirjalili, V., Fong, A., Laird, A.R., Saeed, F.: ASD-DiagNet: a hybrid learning approach for detection of autism spectrum disorder using fMRI data. Front. Neuroinform. **13**, 70 (2019)
3. Gadgil, S., Zhao, Q., Pfefferbaum, A., Sullivan, E.V., Adeli, E., Pohl, K.M.: Spatio-temporal graph convolution for resting-state fMRI analysis. In: Martel, A.L., et al. (eds.) MICCAI 2020. LNCS, vol. 12267, pp. 528–538. Springer, Cham (2020). https://doi.org/10.1007/978-3-030-59728-3_52
4. Imran, A.A.Z., Wang, S., Pal, D., Dutta, S., Zucker, E., Wang, A.: Multimodal contrastive learning for prospective personalized estimation of CT organ dose. In: Wang, L., Dou, Q., Fletcher, P.T., Speidel, S., Li, S. (eds.) MICCAI 2022, Part I. LNCS, vol. 13431, pp. 634–643. Springer, Cham (2022). https://doi.org/10.1007/978-3-031-16431-6_60
5. Kawahara, J., et al.: BrainNetCNN: convolutional neural networks for brain networks; towards predicting neurodevelopment. Neuroimage **146**, 1038–1049 (2017)
6. Khosla, M., Jamison, K., Ngo, G.H., Kuceyeski, A., Sabuncu, M.R.: Machine learning in resting-state fMRI analysis. Magn. Reson. Imaging **64**, 101–121 (2019)
7. Kiranyaz, S., Avci, O., Abdeljaber, O., Ince, T., Gabbouj, M., Inman, D.J.: 1D convolutional neural networks and applications: a survey. Mech. Syst. Sig. Process. **151**, 107398 (2021)
8. Kumar, V., Garg, R.: Resting state functional connectivity alterations in individuals with autism spectrum disorders: a systematic review. medRxiv (2021)
9. Lawry Aguila, A., Chapman, J., Janahi, M., Altmann, A.: Conditional VAEs for confound removal and normative modelling of neurodegenerative diseases. In: Wang, L., Dou, Q., Fletcher, P.T., Speidel, S., Li, S. (eds.) MICCAI 2022, Part I. LNCS, vol. 13431, pp. 430–440. Springer, Cham (2022). https://doi.org/10.1007/978-3-031-16431-6_41
10. Lee, W.H., Frangou, S.: Linking functional connectivity and dynamic properties of resting-state networks. Sci. Rep. **7**(1), 16610 (2017)
11. Lynch, C.J., Uddin, L.Q., Supekar, K., Khouzam, A., Phillips, J., Menon, V.: Default mode network in childhood autism: posteromedial cortex heterogeneity and relationship with social deficits. Biol. Psychiatry **74**(3), 212–219 (2013)
12. Nebel, M.B., et al.: Intrinsic visual-motor synchrony correlates with social deficits in autism. Biol. Psychiatry **79**(8), 633–641 (2016)

13. Radonjić, N.V., et al.: Structural brain imaging studies offer clues about the effects of the shared genetic etiology among neuropsychiatric disorders. Mol. Psychiatry **26**(6), 2101–2110 (2021)
14. Sauty, B., Durrleman, S.: Progression models for imaging data with longitudinal variational auto encoders. In: Wang, L., Dou, Q., Fletcher, P.T., Speidel, S., Li, S. (eds.) MICCAI 2022, Part I. LNCS, vol. 13431, pp. 3–13. Springer, Cham (2022). https://doi.org/10.1007/978-3-031-16431-6_1
15. Seyfioğlu, M.S., et al.: Brain-aware replacements for supervised contrastive learning in detection of Alzheimer's disease. In: Wang, L., Dou, Q., Fletcher, P.T., Speidel, S., Li, S. (eds.) MICCAI 2022, Part I. LNCS, vol. 13431, pp. 461–470. Springer, Cham (2022). https://doi.org/10.1007/978-3-031-16431-6_44
16. Wang, Y., Kang, J., Kemmer, P.B., Guo, Y.: An efficient and reliable statistical method for estimating functional connectivity in large scale brain networks using partial correlation. Front. Neurosci. **10**, 123 (2016)
17. Wang, Z., et al.: Distribution-guided network thresholding for functional connectivity analysis in fMRI-based brain disorder identification. IEEE J. Biomed. Health Inform. **26**(4), 1602–1613 (2021)
18. Wen, G., Cao, P., Bao, H., Yang, W., Zheng, T., Zaiane, O.: MVS-GCN: a prior brain structure learning-guided multi-view graph convolution network for autism spectrum disorder diagnosis. Comput. Biol. Med. **142**, 105239 (2022)
19. Xia, M., Wang, J., He, Y.: BrainNet Viewer: a network visualization tool for human brain connectomics. PLoS ONE **8**(7), e68910 (2013)
20. Yan, C.G., Wang, X.D., Zuo, X.N., Zang, Y.F.: DPABI: data processing & analysis for (resting-state) brain imaging. Neuroinformatics **14**(3), 339–351 (2016). https://doi.org/10.1007/s12021-016-9299-4
21. Yan, K., Zhang, D.: Feature selection and analysis on correlated gas sensor data with recursive feature elimination. Sens. Actuators, B Chem. **212**, 353–363 (2015)
22. Yan, Y., Zhu, J., Duda, M., Solarz, E., Sripada, C., Koutra, D.: GroupINN: grouping-based interpretable neural network for classification of limited, noisy brain data. In: Proceedings of the 25th ACM SIGKDD International Conference on Knowledge Discovery & Data Mining, pp. 772–782 (2019)
23. Yin, W., Li, L., Wu, F.X.: Deep learning for brain disorder diagnosis based on fMRI images. Neurocomputing **469**, 332–345 (2022)
24. You, Y., Chen, T., Sui, Y., Chen, T., Wang, Z., Shen, Y.: Graph contrastive learning with augmentations. In: Advances in Neural Information Processing Systems, vol. 33, pp. 5812–5823 (2020)
25. Zhang, Z., Ding, J., Xu, J., Tang, J., Guo, F.: Multi-scale time-series kernel-based learning method for brain disease diagnosis. IEEE J. Biomed. Health Inform. **25**(1), 209–217 (2020)
26. Zhao, H., Nyholt, D.R.: Gene-based analyses reveal novel genetic overlap and allelic heterogeneity across five major psychiatric disorders. Hum. Genet. **136**, 263–274 (2017). https://doi.org/10.1007/s00439-016-1755-6
27. Zhou, Z.H., Sun, Y.Y., Li, Y.F.: Multi-instance learning by treating instances as non-IID samples. In: Proceedings of the 26th Annual International Conference on Machine Learning, pp. 1249–1256 (2009)
28. Zhu, Y., Xu, W., Zhang, J., Liu, Q., Wu, S., Wang, L.: Deep graph structure learning for robust representations: a survey. arXiv preprint arXiv:2103.03036 (2021)